CURVE SHORTENING FLOW AND THE MAXIMUM PRINCIPLE: AVOIDANCE AND CONVEXITY - A PROJECT SUPERVISED BY PROFESSOR RAPHAEL ZENTNER

JAKUB PICKERING

Abstract. The curve shortening flow (CSF) is the simplest nontrivial example of a geometric flow, evolving a smooth plane curve in the normal direction with speed equal to its curvature. This paper develops the parabolic partial differential equation framework underlying CSF, including the classification of PDEs and the parabolic maximum principle. These analytical tools are then applied to establish two central geometric results: the *avoidance principle*, ensuring that disjoint curves remain disjoint under the flow, and the *preservation of convexity*, showing that convex curves remain convex until they contract to a point. The discussion highlights how parabolic features such as infinite propagation speed and smoothing translate into geometric regularisation. Finally, the broader significance of these results is noted through *Grayson's theorem*, which completes the classification of planar CSF by proving that every embedded curve becomes convex and shrinks to a round point. In this way, the curve shortening flow serves as a link between parabolic PDE theory and geometric evolution. This exposition demonstrates how analytic principles of parabolic PDEs yield profound geometric consequences.

Contents

1. Introduction 3

2. Background on Parabolic PDEs 3

2.1. Basics of PDEs 3

2.2. Classification of Second Order Linear PDEs 4

2.3. Properties of Parabolic PDEs 5

3. The Curve Shortening Flow 9

3.1. Geometric Preliminaries 9

3.2. CSF Definitions and Basic Properties 10

3.3. Analytic Form of the Flow 11

4. Applications of the Maximum Principle 16

4.1. The Avoidance Principle 17

4.2. Preservation of Convexity 19

4.3. Discussion and Further Consequences 21

Date: October 24, 2025.
This exposition was written under the supervision of Professor Raphael Zentner.

5. Infinite Propagation Speed and Smoothing 21

5.1. Infinite propagation speed 21

5.2. Broader significance 22

5.3. Conclusion 22

6. Further Directions – A Note on Grayson's Theorem 22

6.1. Grayson's theorem 23

6.2. Historical note and outlook 23

Acknowledgements 24

References 24

1. Introduction

The study of geometric flows provides deep insights into both analysis and geometry by evolving shapes according to curvature. Among these flows, the *curve shortening flow* (CSF) is the simplest nontrivial case: a smooth embedded curve in the plane moves in the normal direction at a speed equal to its curvature. Despite its apparent simplicity, CSF captures the essential features of more general flows, including mean curvature flow and Hamilton's Ricci flow, and it has applications ranging from geometry to image processing.

From the analytic viewpoint, the curvature evolution equation associated with CSF is a nonlinear *parabolic PDE*. Parabolic equations are diffusion-like: they smooth initial data, exhibit infinite propagation speed, and are governed by powerful tools such as the maximum principle. In the case of CSF, the maximum principle translates directly into important geometric results.

This paper focuses on two such results: the *avoidance principle*, which ensures that disjoint curves remain disjoint as they evolve, and the *preservation of convexity*, which shows that convex curves remain convex until they contract to a point. Both principles are proved using variants of the parabolic maximum principle, highlighting the close connection between PDE theory and geometry. In preparing this exposition, we adopt much of the framework from Chow and Knopf [1].

The paper has the following structure. Section 2 reviews the necessary background on parabolic PDEs, their classification, and the maximum principle. Section 3 introduces the curve shortening flow and derives the curvature evolution equation. Section 4 applies the maximum principle to prove the avoidance principle and the preservation of convexity. Section 5 discusses infinite propagation speed and its geometric significance, before concluding with broader remarks. Finally, Section 6 concludes the paper with further directions and a discussion of Grayson's theorem, which provides a complete classification of embedded planar curves under the flow.

2. Background on Parabolic PDEs

2.1. **Basics of PDEs.** Before specialising to parabolic equations, it is useful to state the general definition of a partial differential equation. In broad terms, a PDE specifies a relation among a function, its derivatives, and the point at which they are evaluated. More precisely:

Definition 2.1. For $U \subseteq \mathbb{R}^n$ open, a PDE of **order k** is a relation of form:

$$F(x, u(x), Du(x), D^2u(x), \ldots, D^k u(x)) = 0$$

where $D^k u(x)$ is the full collection of kth order partial derivatives at the point x, and

$$F : U \times \mathbb{R} \times \mathbb{R}^n \times \mathbb{R}^{n^2} \times \cdots \times \mathbb{R}^{n^k} \to \mathbb{R}$$

is a given function and u is to be found, known as the dependent variable.

Remark 2.2. Although PDEs can be defined in very general terms, we shall concentrate on the subclass of linear PDEs, which are more amenable to analysis.

Definition 2.3. A PDE is said to be linear if it is linear in the dependent variable u

Example 2.4. Our favourite example of a PDE the Heat Equation discovered by Joseph Fourier in 1807 is a linear partial differential equation.

$$\frac{\partial u}{\partial t} = \Delta u$$

The *order* of a PDE is determined by the highest derivative of u that appears. For example, the *transport equation*

$$u_t + cu_x = 0$$

is a *first-order* linear PDE, whereas the *wave equation*

$$u_{tt} - c^2 u_{xx} = 0$$

is a *second-order* linear PDE. These examples already illustrate why second-order equations occupy a central role: many of the most fundamental models in physics and geometry belong to this class.

Having established the general framework and introduced the notion of linearity, we now turn our attention to the most important case for applications: *second-order linear PDEs*. These equations arise naturally in physics, geometry, and probability, describing phenomena such as heat flow, wave propagation, and potential theory. A central feature of second-order linear PDEs is that their behavior can be understood through a classification of the underlying differential operator. This classification, which divides equations into elliptic, parabolic, and hyperbolic types, plays a crucial role in guiding the appropriate analytical techniques and in interpreting the qualitative nature of solutions.

2.2. **Classification of Second Order Linear PDEs.** We have already discussed the importance of second order linear PDEs in Analysis and Applied Mathematics. We can write such a PDE in the following form:

$$Au_{xx} + Bu_{xy} + Cu_{yy} + Du_x + Eu_y + Fu = G$$

where our coefficients are general functions of the independent variables x and y. We want to classify this class of PDEs. This only depends on the *second order terms*, so for convenience we rewrite this as:

$$Au_{xx} + Bu_{xy} + Cu_{yy} + I(x, y, u, u_x, u_y) = 0$$

We can check that this only depends on the sign of the quantity:

$$\Delta(x, y) = B^2(x, y) - 4A(x, y)C(x, y)$$

The so called *discriminant* of our PDE. It is with this quantity that we classify second order linear PDEs.

Definition 2.5 (Classification of PDEs)**.** At the point (x_0, y_0) the second order linear PDE is called:

- **Hyperbolic** if $\Delta(x_0, y_0) > 0$
- **Parabolic** if $\Delta(x_0, y_0) = 0$
- **Elliptic** if $\Delta(x_0, y_0) < 0$

Although the classification of second-order linear PDEs is algebraic in nature, its true significance lies in the very different analytic behaviours of the resulting equations. To illustrate this, we present the canonical examples of each class.

Example 2.6 (Elliptic: Laplace's equation)**.**

$$u_{xx} + u_{yy} = 0.$$

This is the prototypical elliptic PDE. It models steady–state phenomena such as electrostatics, incompressible fluid flow, and potential theory. Solutions are typically smooth and determined entirely by boundary conditions.

Example 2.7 (Parabolic: Heat equation)**.**

$$u_t - u_{xx} = 0.$$

This is the standard parabolic PDE, describing diffusion and smoothing. Information propagates instantly, but regularity improves over time. This smoothing effect is a hallmark of parabolic equations and will be central in our study of curve shortening flow.

Example 2.8 (Hyperbolic: Wave equation)**.**

$$u_{tt} - c^2 u_{xx} = 0.$$

This is the canonical hyperbolic PDE. It governs waves and signals with finite propagation speed (such as sound or light), preserving oscillations rather than smoothing them out.

Having introduced the classification of second-order linear PDEs, we now turn our attention to the parabolic case. Parabolic equations are distinguished by their smoothing effect and infinite propagation speed, features that play a crucial role in geometric flows. Since the curve shortening flow is governed by a nonlinear parabolic PDE, it is natural to first investigate the key properties of parabolic equations in general.

2.3. **Properties of Parabolic PDEs.** An essential feature of parabolic PDEs is that their solutions exhibit strong monotonicity properties, reflecting the diffusive and smoothing character of these equations. These properties are formalised in the maximum principles, which state, roughly speaking, that the extreme values of a solution are controlled by its initial and boundary data. We begin by recalling the weak maximum principle, which provides a basic form of this control, and then strengthen it to the strong maximum principle, which plays a crucial role in the analysis of geometric flows such as CSF. Both principles will be used repeatedly in the proofs concerning curve shortening flow, making them indispensable for the analysis to follow.

Theorem 2.9 (Weak Maximum Principle)**.** *Let* $u \in C^2(\Omega_T) \cap C(\overline{\Omega_T})$ *satisfy*

$$u_t - \Delta u \leq 0 \quad \textit{in } \Omega_T$$

then:

$$\max_{\overline{\Omega_T}} u = \max_{\partial_p \Omega_T} u$$

Proof. **Step 1:** Assume u is such that $u_t - u_{xx} < 0$ in Ω_t.

Claim: The maximum of u is only achieved on $\partial\Omega_T$.

Proof of claim: As $\overline{\Omega_T}$ is bounded and closed it is therefore compact, and since u is continuous we have that $\exists p^* = (x^*, t^*) \in \overline{\Omega_T}$ such that

$$u(p^*) = \max_{\overline{\Omega_T}} u$$

We now want to exclude the possibility of achieving our maximum on the interior or on the top boundary $\{t = T\}$. Suppose $p^* \notin \partial_p\Omega_T$, then either:

(1) $p^* = (x^*, t^*) \in \Omega_T$ with $t^* < T$

(2) $p^* = (x^*, t^*) \in \overline{\Omega_T}$ with $t^* = T$

In both situations we have that $x \to u(x, t^*)$ achieves a maximum at $x = x^*$. Therefore $u_x(p^*) = 0$ and also $u_{xx}(p^*) \leq 0$. Now we examine the two cases separately.

(1) In the first case, since $p^* = (x^*, t^*)$ is an interior spacetime maximum with $t^* < T$, we must have $u_t(p^*) = 0$ (as a critical point in time), $u_x(p^*) = 0$, and $u_{xx}(p^*) \leq 0$.

Therefore, $u_t(p^*) - u_{xx}(p^*) \geq 0$, which contradicts our assumption that $u_t - u_{xx} < 0$ in Ω_T.

(2) In the second case, we have $p^* = (x^*, T)$ where $x^* \in \Omega$. At this point, $u_x(p^*) = 0$ and $u_{xx}(p^*) \leq 0$.

From the PDE, we have

$$u_t(x^*, T) \leq u_{xx}(x^*, T) \leq 0$$

This means u is non-increasing in time at (x^*, T). Therefore, for t slightly less than T:

$$u(x^*, t) \geq u(x^*, T) \quad \text{for } t < T \text{ near } T$$

This contradicts the assumption that u achieves a strict maximum at (x^*, T).

Therefore in both cases we obtain a contradiction. Hence the maximum must be attained on the parabolic boundary $\partial_p\Omega_T$.

Step 2: Let u be such that $u_t - u_{xx} \leq 0$ in Ω_T.

Define the modified function

$$u_\varepsilon(x, t) := u(x, t) - \varepsilon t, \quad \varepsilon > 0$$

Then

$$(u_\varepsilon)_t - (u_\varepsilon)_{xx} = u_t - u_{xx} - \varepsilon < 0$$

so u_ε satisfies the strict inequality.

By Step 1, we know

$$\max_{\overline{\Omega_T}} u_\varepsilon = \max_{\partial_p \Omega_T} u_\varepsilon$$

Now,

$$\max_{\partial_p \Omega_T} u \geq \max_{\partial_p \Omega_T} u_\varepsilon = \max_{\overline{\Omega_T}} u_\varepsilon \geq \max_{\overline{\Omega_T}} (u - \varepsilon T)$$

Thus,

$$\max_{\overline{\Omega_T}} u \leq \max_{\partial_p \Omega_T} u + \varepsilon T$$

Finally, taking $\varepsilon \to 0$ gives the claim of equality:

$$\max_{\overline{\Omega_T}} u = \max_{\partial_p \Omega_T} u$$

□

The weak maximum principle shows that the extrema of a single solution are attained on the parabolic boundary. By applying this to the difference $w = u - v$ of two functions, where u is a subsolution and v is a supersolution, we obtain the *comparison principle*. This states that if $u \leq v$ initially and on the spatial boundary, then the inequality persists throughout the domain for all positive times.

Corollary 2.10 (Parabolic Comparison Principle)**.** *Let $u, v \in C^{2,1}(\Omega_T) \cap C(\overline{\Omega_T})$, where $\Omega_T = \Omega \times (0, T]$ and $\Omega \subset \mathbb{R}^n$ is bounded.*

Suppose

$$u_t - \Delta u \leq 0 \quad \text{in } \Omega_T, \qquad v_t - \Delta v \geq 0 \quad \text{in } \Omega_T,$$

that is, u is a subsolution and v is a supersolution of the heat equation.

If

$$u(x, 0) \leq v(x, 0) \quad \text{for all } x \in \Omega,$$

and

$$u \leq v \quad \text{on } \partial\Omega \times (0, T],$$

then

$$u(x, t) \leq v(x, t) \quad \text{for all } (x, t) \in \Omega_T.$$

Sketch of proof. Consider the difference $w = u - v$. Then

$$w_t - \Delta w \leq 0 \quad \text{in } \Omega_T,$$

and $w \leq 0$ on the parabolic boundary Γ_{Ω_T}. The weak maximum principle applied to w implies that $w \leq 0$ throughout Ω_T, which is exactly the desired inequality $u \leq v$. □

The weak maximum principle guarantees that the maximum and minimum values of a solution occur on the boundary of the domain, but it does not rule out the possibility that such extrema are also attained at interior points. To sharpen this conclusion, we require the *strong maximum principle*, which shows that nontrivial interior extrema cannot occur unless the solution is

constant. This stronger result will be especially important in the context of curve shortening flow, where ruling out interior maxima and minima underlies many of the key proofs.

Theorem 2.11 (Strong Maximum Principle)**.** *Let $u \in C^2(\Omega_T) \cap C(\overline{\Omega_T})$ satisfy*

$$u_t - \Delta u \leq 0 \quad \text{in } \Omega_T.$$

If Ω is connected and there exists $(x_0, t_0) \in \Omega_T$ such that

$$u(x_0, t_0) = \max_{\overline{\Omega_T}} u,$$

then u is constant in $\overline{\Omega_{t_0}}$.

Proof. The proof is omitted here and can be found in standard PDE references, see for instance Evans [2, Chapter 7] or Lieberman [5, Chapter 2]. □

The maximum principles already highlight one of the most striking aspects of parabolic equations: their solutions are heavily constrained by boundary and initial data. Yet, beyond these extremal properties, parabolic equations exhibit another remarkable feature: information propagates instantaneously. In other words, any local disturbance in the initial data is felt everywhere in the domain for all later times. This phenomenon, known as *infinite propagation speed*, sharply contrasts with the finite-speed propagation of hyperbolic equations and will play a central role in understanding the geometric behavior of curve shortening flow.

Theorem 2.12 (Infinite Propagation Speed)**.** *Let $\Omega \subset \mathbb{R}^n$ be open, bounded, smooth and connected. Let $T > 0$, $g : \overline{\Omega} \to \mathbb{R}$ be continuous and $u \in C^2(\Omega_T) \cap C(\overline{\Omega_T})$ satisfy*

$$\begin{cases} u_t - \Delta u = 0 & \text{in } \Omega_T \\ u = 0 & \text{on } \partial\Omega_T \times [0, T] \\ u = g & \text{on } \Omega \times \{t = 0\} \end{cases}$$

If $g > 0$ somewhere in Ω then $u \geq 0$ everywhere in Ω_T

Proof. Since u satisfies the heat equation, we also have that $u_t - \Delta u \geq 0$ (ie this is a supersolution to the heat equation) and so we can use both the parabolic strong and weak *minimum* principles. But since $g \geq 0$, we have

$$\min_{\Gamma_{\Omega_T}} u = 0.$$

Thus the parabolic weak minimum principle implies $u \geq 0$ in Ω_T. On the other hand, if $u(x, t) = 0$ for some $(x, t) \in \Omega_T$, the parabolic strong minimum principle would imply that

$$u \equiv 0 \qquad \text{in } \overline{\Omega}_t.$$

But this would imply

$$u \equiv 0 \qquad \text{on } \Omega \times \{t = 0\}.$$

But this contradicts the fact that $g > 0$ somewhere in Ω. So indeed we see that $u \geq 0$ everywhere in Ω_T □

To summarise, parabolic PDEs are distinguished by two key analytic features. First, they exhibit *infinite propagation speed*, whereby any local disturbance immediately influences the entire domain. Second, their behaviour is governed by the *maximum principle*, which restricts where extrema can occur, and by the *comparison principle*, which guarantees that the relative ordering of two solutions is preserved for all later times.

These principles will play a central role in our study of the curve shortening flow. In the geometric setting, the comparison principle becomes the *avoidance principle*, ensuring that initially disjoint curves remain disjoint as they evolve, while the strong maximum principle underlies the preservation of convexity. We now turn to the definition of the curve shortening flow and the derivation of its governing equation.

3. The Curve Shortening Flow

3.1. **Geometric Preliminaries.** Before introducing the curve shortening flow, we recall some basic notions from the differential geometry of plane curves.

Definition 3.1 (Immersed Curve)**.** An **immersed curve** is a smooth map $\gamma : I \to \mathbb{R}^2$ (where I is an interval) such that the derivative $|\gamma'(t)| \neq 0$ for all $t \in I$. This means the curve has a well-defined tangent vector at every point and no "stopping" or "cusps."

Definition 3.2. An **embedded curve** is an immersed curve that is a homeomorphism onto its image (when the image has the subspace topology). In simpler terms, an embedded curve doesn't intersect itself at all.

Remark 3.3. The crucial distinction is:

- **Immersed**: Tangent vector is defined everywhere and self-intersections are allowed.
- **Embedded**: No self-intersections at all-the curve is a faithful copy of the interval in the manifold.

An intuitive way to think of this would be if you were walking along an immersed curve, you'd always be moving forward (never stopping), but you might cross your own path. On an embedded curve, you'd never cross your own path.

Definition 3.4 (Arc length parametrisation)**.** Let $\gamma : S^1 \to \mathbb{R}^2$ be a smooth immersed closed curve. If u is a parameter on S^1, then the arc length s is given by

$$s(u) = \int_{u_0}^{u} |\gamma'(v)|\, dv.$$

When γ is parametrised by arc length, we have $|\gamma_s| = 1$, where $\gamma_s = \frac{\partial \gamma}{\partial s}$.

Definition 3.5 (Unit tangent and normal)**.** For a curve $\gamma(s)$ parametrised by arc length s, the unit tangent vector is

$$T(s) = \frac{\partial \gamma}{\partial s} = \gamma_s(s), \qquad |T(s)| = 1.$$

The inward unit normal vector $\nu(s)$ is defined so that $\{T(s), \nu(s)\}$ forms an orthonormal positively oriented basis of $\mathbb{R}^2$.

Definition 3.6 (Curvature)**.** The curvature $\kappa(s)$ of γ at the point $\gamma(s)$ is defined by

$$\frac{dT}{ds} = \kappa\,\nu.$$

Equivalently, since γ_{ss} is orthogonal to T, one has

$$\gamma_{ss} = \kappa\nu.$$

The curvature is taken to be positive when the curve bends in the direction of the inward normal ν.

These basic geometric identities, known as the Frenet–Serret formulas in the planar case, will be essential for describing the curve shortening flow and for deriving evolution equations for geometric quantities such as curvature, length, and enclosed area.

3.2. **CSF Definitions and Basic Properties.** Having established the basic notions of tangent, normal, and curvature, we now introduce the *curve shortening flow* (CSF). This is the simplest example of a geometric evolution equation: a closed plane curve evolves in such a way that each point moves in the inward normal direction with velocity equal to the curvature at that point. Regions of high curvature contract more rapidly than flatter regions, and as a result the flow tends to smooth out irregularities in the curve. From the analytic viewpoint, CSF is a nonlinear parabolic equation, often regarded as the "heat equation for curves," since it has diffusion-like properties. We begin with a precise definition.

Definition 3.7 (Curve Shortening Flow)**.** Let $\gamma_0 : S^1 \to \mathbb{R}^2$ be a smooth, embedded closed curve. The *curve shortening flow (CSF)* is a one-parameter family of smooth immersions

$$\gamma : S^1 \times [0,T) \to \mathbb{R}^2, \qquad (s,t) \mapsto \gamma(s,t),$$

such that

(1) $\gamma(\cdot,0) = \gamma_0$, and

(2) the family evolves according to the law

$$\frac{\partial\gamma(s,t)}{\partial t} = \kappa(s,t)\,\nu(s,t),$$

where $\kappa(s,t)$ is the curvature of γ at (s,t) and $\nu(s,t)$ is the inward-pointing unit normal. Equivalently, if γ is parametrised by arc length s, then

$$\kappa(s,t) = \frac{d^2\gamma}{ds^2} \cdot \nu(s,t).$$

To build intuition for the definition, it is helpful to examine some simple examples of curves evolving under CSF. The most natural starting point is the circle: its symmetry makes the evolution easy to describe explicitly, and it already illustrates many of the key features of the flow. In particular, we will see that a circle remains a circle under the flow, its radius decreases according to a simple ODE, and it shrinks smoothly to a round point in finite time.

Example 3.8 (Circle under CSF)**.** Let $\gamma_0(\theta) = (R_0\cos\theta, R_0\sin\theta)$ be a circle of radius R_0. For a circle of radius R, the curvature is constant $\kappa = 1/R$, and the inward normal is radial. Thus

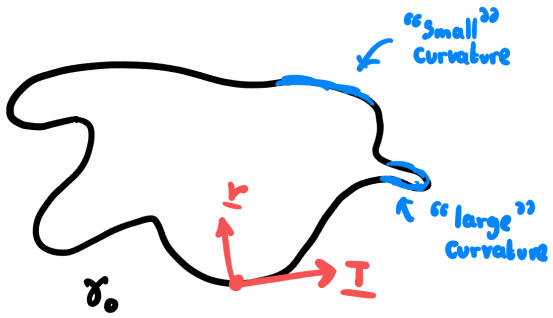

FIGURE 1. A smooth embedded curve γ_0 with tangent T and normal ν. Regions of small and large curvature are highlighted.

the flow preserves the circular shape, and only the radius changes over time. If $R(t)$ denotes the radius at time t, then

$$\frac{dR}{dt} = -\frac{1}{R(t)}.$$

Solving this ODE gives

$$R(t) = \sqrt{R_0^2 - 2t},$$

so the circle collapses to a point at time $T = R_0^2/2$. The length and area are

$$L(t) = 2\pi R(t), \qquad A(t) = \pi R(t)^2,$$

with $\frac{d}{dt}A(t) = -2\pi$. Thus a circle contracts smoothly and remains round until it vanishes in finite time.

3.3. **Analytic Form of the Flow.** We now seek to see how our different geometric quantities evolve in time under CSF.

Theorem 3.9 (Curvature Evolution Equation)**.** *Under Curve Shortening Flow , the curvature evolves according to*

$$\frac{\partial \kappa}{\partial t} = \frac{\partial^2 \kappa}{\partial s^2} + \kappa^3.$$

Proof. The proof proceeds in several steps: we first compute how the moving frame evolves in time, then use compatibility conditions from mixed partial derivatives.

Step 1: Evolution of the tangent vector

Lemma 3.10. *The tangent vector evolves according to*

$$\frac{\partial \mathbf{T}}{\partial t} = \frac{\partial \kappa}{\partial s}\boldsymbol{\nu}.$$

Proof. Since $\mathbf{T} = \frac{\partial \gamma}{\partial s}$ and mixed partial derivatives commute and using CSF, we have

$$\frac{\partial \mathbf{T}}{\partial t} = \frac{\partial}{\partial t}\left(\frac{\partial \gamma}{\partial s}\right) = \frac{\partial}{\partial s}\left(\frac{\partial \gamma}{\partial t}\right) = \frac{\partial}{\partial s}(\kappa \boldsymbol{\nu}) = \frac{\partial \kappa}{\partial s}\boldsymbol{\nu} + \kappa \frac{\partial \boldsymbol{\nu}}{\partial s}$$

Using the Frenet-Serret formula we finally have:

$$\frac{\partial \mathbf{T}}{\partial t} = \frac{\partial \kappa}{\partial s}\boldsymbol{\nu} - \kappa^2 \mathbf{T}.$$

Now, since $\mathbf{T}$ is a unit vector, we have $\mathbf{T} \cdot \mathbf{T} = 1$. Differentiating with respect to t:

$$2\mathbf{T} \cdot \frac{\partial \mathbf{T}}{\partial t} = 0.$$

This shows that $\frac{\partial \mathbf{T}}{\partial t}$ is perpendicular to $\mathbf{T}$, so it must be proportional to $\boldsymbol{\nu}$:

$$\frac{\partial \mathbf{T}}{\partial t} = \alpha \boldsymbol{\nu}$$

for some scalar function $\alpha(s, t)$.

Comparing, the normal component gives:

$$\alpha = \frac{\partial \kappa}{\partial s},$$

while the tangent component gives $0 = -\kappa^2$, which appears contradictory.

The resolution is that we must account for the fact that the arc-length parametrisation changes with time. However, for the normal component (which is what we need), we correctly obtain our equation. □

Step 2: Evolution of the normal vector

Lemma 3.11. *The normal vector evolves according to*

$$\frac{\partial \boldsymbol{\nu}}{\partial t} = -\frac{\partial \kappa}{\partial s}\mathbf{T}.$$

Proof. Since $\boldsymbol{\nu}$ is a unit vector, $\boldsymbol{\nu} \cdot \boldsymbol{\nu} = 1$, which gives:

$$2\boldsymbol{\nu} \cdot \frac{\partial \boldsymbol{\nu}}{\partial t} = 0.$$

Thus $\frac{\partial \boldsymbol{\nu}}{\partial t}$ is perpendicular to $\boldsymbol{\nu}$, so:

$$\frac{\partial \boldsymbol{\nu}}{\partial t} = \beta \mathbf{T}$$

for some scalar β.

Since $\mathbf{T} \cdot \boldsymbol{\nu} = 0$, differentiating with respect to t:

$$\frac{\partial \mathbf{T}}{\partial t} \cdot \boldsymbol{\nu} + \mathbf{T} \cdot \frac{\partial \boldsymbol{\nu}}{\partial t} = 0.$$

Substituting our expressions and using Lemma 3.10:

$$\left(\frac{\partial \kappa}{\partial s}\boldsymbol{\nu}\right) \cdot \boldsymbol{\nu} + \mathbf{T} \cdot (\beta \mathbf{T}) = 0,$$

$$\frac{\partial \kappa}{\partial s} + \beta = 0.$$

Therefore $\beta = -\frac{\partial \kappa}{\partial s}$, giving our result. □

Step 3: Computing mixed derivatives of T

We now use the compatibility condition that mixed partial derivatives must commute.

Starting with the Frenet-Serret formula:

$$\frac{\partial \mathbf{T}}{\partial s} = \kappa \boldsymbol{\nu}.$$

Differentiate with respect to t:

$$\frac{\partial^2 \mathbf{T}}{\partial t \partial s} = \frac{\partial}{\partial t}(\kappa \boldsymbol{\nu}) = \frac{\partial \kappa}{\partial t}\boldsymbol{\nu} + \kappa \frac{\partial \boldsymbol{\nu}}{\partial t}.$$

Using equation our lemma:

$$\frac{\partial^2 \mathbf{T}}{\partial t \partial s} = \frac{\partial \kappa}{\partial t}\boldsymbol{\nu} - \kappa \frac{\partial \kappa}{\partial s}\mathbf{T}.$$

Now compute in the opposite order. From our lemma again:

$$\frac{\partial \mathbf{T}}{\partial t} = \frac{\partial \kappa}{\partial s}\boldsymbol{\nu}.$$

Differentiate with respect to s:

$$\frac{\partial^2 \mathbf{T}}{\partial s \partial t} = \frac{\partial}{\partial s}\left(\frac{\partial \kappa}{\partial s}\boldsymbol{\nu}\right) = \frac{\partial^2 \kappa}{\partial s^2}\boldsymbol{\nu} + \frac{\partial \kappa}{\partial s}\frac{\partial \boldsymbol{\nu}}{\partial s}.$$

Using equation our Frenet-Serret Equations:

$$\frac{\partial^2 \mathbf{T}}{\partial s \partial t} = \frac{\partial^2 \kappa}{\partial s^2}\boldsymbol{\nu} - \kappa \frac{\partial \kappa}{\partial s}\mathbf{T}.$$

Step 4: Equating mixed derivatives

By equality of mixed partial derivatives:

$$\frac{\partial^2 \mathbf{T}}{\partial t \partial s} = \frac{\partial^2 \mathbf{T}}{\partial s \partial t}.$$

Then:

$$\frac{\partial \kappa}{\partial t}\boldsymbol{\nu} - \kappa \frac{\partial \kappa}{\partial s}\mathbf{T} = \frac{\partial^2 \kappa}{\partial s^2}\boldsymbol{\nu} - \kappa \frac{\partial \kappa}{\partial s}\mathbf{T}.$$

The tangent components are identical on both sides (both equal $-\kappa \frac{\partial \kappa}{\partial s}$).

Comparing the normal components:

$$\frac{\partial \kappa}{\partial t} = \frac{\partial^2 \kappa}{\partial s^2}.$$

Step 5: Accounting for arc-length evolution

Our last equation is not yet complete. We must account for the fact that the arc-length parametrisation itself evolves with time.

The length element ds changes according to:

Lemma 3.12 (Evolution of Arc-Length Element)**.** *Under the flow $\gamma_t = \kappa\boldsymbol{\nu}$, the arc-length element evolves according to*

$$\frac{\partial}{\partial t}(ds) = -\kappa^2\, ds.$$

Proof. Let u be a fixed parameter for the curve. At time t, the arc-length element is $ds = \left|\frac{\partial\gamma}{\partial u}\right| du$. Since $\mathbf{T} = \frac{\partial\gamma}{\partial s}$, we have

$$\frac{\partial\gamma}{\partial u} = \frac{\partial\gamma}{\partial s}\frac{\partial s}{\partial u} = \mathbf{T}\frac{\partial s}{\partial u},$$

and therefore

$$\left|\frac{\partial\gamma}{\partial u}\right| = \frac{\partial s}{\partial u}$$

since $\mathbf{T}$ is a unit vector. We now compute:

$$\frac{\partial}{\partial t}\left(\frac{\partial s}{\partial u}\right) = \frac{\partial}{\partial t}\left|\frac{\partial\gamma}{\partial u}\right|.$$

Using the formula for the derivative of a norm,

$$\frac{\partial}{\partial t}|\mathbf{v}| = \frac{\mathbf{v}\cdot\frac{\partial\mathbf{v}}{\partial t}}{|\mathbf{v}|}$$

We get

$$\frac{\partial}{\partial t}\left|\frac{\partial\gamma}{\partial u}\right| = \frac{1}{\left|\frac{\partial\gamma}{\partial u}\right|}\frac{\partial\gamma}{\partial u}\cdot\frac{\partial^2\gamma}{\partial t\partial u}.$$

Since $\frac{\partial\gamma}{\partial u} = \mathbf{T}\frac{\partial s}{\partial u}$ and $\left|\frac{\partial\gamma}{\partial u}\right| = \frac{\partial s}{\partial u}$ We get

$$\frac{\partial}{\partial t}\left|\frac{\partial\gamma}{\partial u}\right| = \mathbf{T}\cdot\frac{\partial^2\gamma}{\partial t\partial u}.$$

From the CSF equation:

$$\frac{\partial^2\gamma}{\partial t\partial u} = \frac{\partial}{\partial u}(\kappa\boldsymbol{\nu}) = \frac{\partial\kappa}{\partial u}\boldsymbol{\nu} + \kappa\frac{\partial\boldsymbol{\nu}}{\partial u}.$$

Converting to arc-length derivatives:

$$= \frac{\partial\kappa}{\partial s}\frac{\partial s}{\partial u}\boldsymbol{\nu} + \kappa\frac{\partial\boldsymbol{\nu}}{\partial s}\frac{\partial s}{\partial u} = \frac{\partial s}{\partial u}\left(\frac{\partial\kappa}{\partial s}\boldsymbol{\nu} + \kappa\frac{\partial\boldsymbol{\nu}}{\partial s}\right).$$

Using the Frenet-Serret formula $\frac{\partial\boldsymbol{\nu}}{\partial s} = -\kappa\mathbf{T}$ we get

$$= \frac{\partial s}{\partial u}\left(\frac{\partial\kappa}{\partial s}\boldsymbol{\nu} - \kappa^2\mathbf{T}\right).$$

Taking the dot product with $\mathbf{T}$ and using that $\mathbf{T}\cdot\boldsymbol{\nu} = 0$ and $\mathbf{T}\cdot\mathbf{T} = 1$:

$$\mathbf{T}\cdot\frac{\partial^2\gamma}{\partial t\partial u} = \frac{\partial s}{\partial u}\left(\frac{\partial\kappa}{\partial s}(\mathbf{T}\cdot\boldsymbol{\nu}) - \kappa^2(\mathbf{T}\cdot\mathbf{T})\right) = -\kappa^2\frac{\partial s}{\partial u}..$$

Therefore we have:

$$\frac{\partial}{\partial t}\left(\frac{\partial s}{\partial u}\right) = -\kappa^2\frac{\partial s}{\partial u}.$$

Multiplying both sides by du yields the desired result. □

So for a curve evolving by $\gamma_t = \kappa\boldsymbol{\nu}$,

$$\frac{\partial}{\partial t}\left(\frac{\partial s}{\partial u}\right) = -\kappa^2 \frac{\partial s}{\partial u}.$$

This introduces a correction term when converting time derivatives from the fixed parametrisation to the moving arc-length parametrisation. The correction gives an additional κ^3 term.

More precisely, if $\tilde{\kappa}$ denotes curvature with respect to a fixed parametrisation and κ with respect to the evolving arc-length, then:

$$\frac{\partial \kappa}{\partial t} = \frac{\partial \tilde{\kappa}}{\partial t} + \kappa^3.$$

Since $\frac{\partial \tilde{\kappa}}{\partial t} = \frac{\partial^2 \kappa}{\partial s^2}$ from our calculation above, we obtain:

$$\frac{\partial \kappa}{\partial t} = \frac{\partial^2 \kappa}{\partial s^2} + \kappa^3.$$

This completes the proof. □

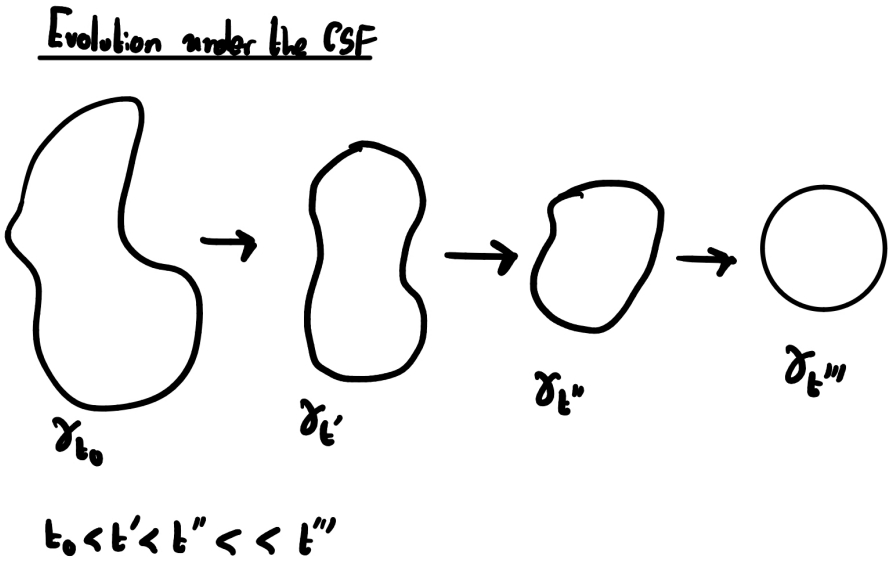

FIGURE 2. The qualitative behaviour of the curve-shortening flow. A closed embedded curve becomes progressively rounder as high-curvature regions contract faster, eventually converging to a circular point in finite time.

Remark 3.13 (Parabolic character of the curvature evolution equation). The curvature evolution equation

$$\frac{\partial \kappa}{\partial t} = \kappa_{ss} + \kappa^3$$

is a *nonlinear parabolic partial differential equation.* The second–derivative term κ_{ss} plays the same analytical role as the Laplacian in the heat equation, producing a *diffusive* effect that smooths variations in curvature along the curve. The cubic term κ^3, by contrast, amplifies regions of high curvature, driving the curve to contract more rapidly where it bends most tightly. Together, these two effects imply that the curve shortening flow acts like a "heat equation for curves": irregularities in shape are smoothed out over time, and the curve evolves toward a more uniform, round geometry before vanishing in finite time.

Corollary 3.14 (Monotonicity of length and area under CSF)**.** *Let γ_t be a smooth family of closed curves evolving by curve shortening flow,*

$$\partial_t \gamma = \kappa \nu.$$

Then the total length $L(t)$ and the enclosed area $A(t)$ satisfy

$$\frac{dL}{dt} = -\int_{\gamma_t} \kappa^2 \, ds \leq 0, \qquad \frac{dA}{dt} = -\int_{\gamma_t} \kappa \, ds = -2\pi.$$

In particular, the length of the curve decreases strictly over time unless the curve is a straight line, and the enclosed area decreases at a constant rate of 2π.

Proof. Differentiating the length functional $L(t) = \int_{\gamma_t} ds$ and using $\partial_t ds = -\kappa^2 ds$ gives

$$\frac{dL}{dt} = \int_{\gamma_t} \partial_t(ds) = -\int_{\gamma_t} \kappa^2 \, ds.$$

Similarly, if γ_t is oriented anti-clockwise with inward normal ν, the rate of change of the enclosed area $A(t)$ is

$$\frac{dA}{dt} = \int_{\gamma_t} \partial_t \gamma \cdot \nu \, ds = \int_{\gamma_t} \kappa \, ds.$$

By the planar Gauss–Bonnet theorem, $\int_{\gamma_t} \kappa \, ds = 2\pi$ for any embedded closed curve, and the chosen orientation introduces a minus sign. Hence $\dfrac{dA}{dt} = -2\pi$. □

Remark 3.15 (Geometric interpretation). The preceding corollary shows that the curve shortening flow is intrinsically contractive: the total length decreases strictly over time, while the enclosed area shrinks at a constant rate. In particular, any smooth embedded curve evolves by continuously reducing its geometric complexity until it collapses to a point in finite time. This monotone behaviour mirrors the diffusive character of the curvature equation, emphasising the close relationship between the analytic and geometric viewpoints.

Having established the fundamental analytic and geometric properties of the curve shortening flow, we are now in a position to apply the *parabolic maximum principle* introduced in Section 2. In the next section, we use this tool to prove two central results: the **avoidance principle**, which guarantees that disjoint curves remain disjoint under the flow, and the **preservation of convexity**, which shows that convex curves remain convex until they contract to a round point.

4. Applications of the Maximum Principle

The analytical framework developed in Section 2 and the geometric formulation of the curve shortening flow in Section 3 now come together. Since the curvature $\kappa(s,t)$ satisfies the nonlinear parabolic equation

$$\partial_t \kappa = \kappa_{ss} + \kappa^3,$$

the powerful tools available for parabolic PDEs—in particular, the maximum principle and its comparison corollaries—can be used to deduce strong geometric consequences. In this section we apply these ideas to prove two fundamental results:

- the **avoidance principle**, which ensures that initially disjoint embedded curves remain disjoint under CSF, and
- the **preservation of convexity**, which states that convex curves remain convex until they contract to a single point.

Both results illustrate how analytic properties of parabolic equations translate into geometric invariants of the evolving curve.

4.1. **The Avoidance Principle.** We now turn to the first geometric consequence of the parabolic maximum principle. Among the most fundamental questions about curve shortening flow is whether two distinct curves can ever develop an intersection as they evolve.

Question Given two smooth embedded curves $\gamma_i(x,t)$ and $\gamma_j(x',t')$ evolving by curve shortening flow, with $i \neq j$, can they intersect at some later time $t > 0$ even if they are initially disjoint?

Answer No. Once disjoint, they remain disjoint for all future times while both flows exist.

This property, known as the *avoidance principle*, is the geometric analogue of the parabolic comparison principle. Just as two distinct solutions of a parabolic PDE cannot cross, two evolving curves under CSF cannot newly intersect. We will now state this result precisely and outline its proof, to do this we will need some lemmas.

Let $\gamma_i(\cdot,t) : S^1 \to \mathbb{R}^2$ $(i = 0, 1)$ be smooth curves. Write $T_i = \partial_s \gamma_i$ for the unit tangent (with respect to arc-length s), ν_i for the unit normal, and κ_i for the signed curvature, so that

$$\partial_s T_i = \kappa_i \nu_i, \qquad \partial_s \nu_i = -\kappa_i T_i.$$

For $x, y \in S^1$ define

$$\Phi(x,y,t) := \frac{1}{2}\big|\gamma_1(y,t) - \gamma_0(x,t)\big|^2, \qquad d(t) := \min_{x,y \in S^1} |\gamma_1(y,t) - \gamma_0(x,t)|.$$

Lemma 4.1 (Existence and geometry of a minimising pair)**.** *For each fixed t, the minimum defining $d(t)$ is attained at some $(x_t, y_t) \in S^1 \times S^1$. Let $w := \gamma_1(y_t,t) - \gamma_0(x_t,t)$. At such a minimising pair we have*

$$\langle w,\, T_0(x_t,t)\rangle = \langle w,\, T_1(y_t,t)\rangle = 0,$$

so that w is perpendicular to both tangents T_0 and T_1. Hence the tangents are parallel and the segment w lies along their common normal direction. Orient the normals so that

$$\nu_0(x_t,t) = \nu_1(y_t,t) = \frac{w}{|w|}.$$

Proof. Continuity of $\Phi(\cdot,\cdot,t)$ on compact $S^1 \times S^1$ ensures existence of a minimiser. Differentiating Φ with respect to x and y at (x_t, y_t) and setting the derivatives to zero yields the stated orthogonality relations. □

Lemma 4.2 (Curvature comparison at a minimising pair)**.** *At any minimising pair (x_t, y_t) for $\Phi(\cdot,\cdot,t)$,*

$$\kappa_1(y_t,t) \;\geq\; \kappa_0(x_t,t).$$

Proof. Parameterise near x_t and y_t by arc-length s and σ. Using $\partial_s T_i = \kappa_i \nu_i$ and Lemma 4.1, we compute at (x_t, y_t, t):

$$\partial_{ss}\Phi + \partial_{\sigma\sigma}\Phi = \langle w,\, \kappa_1\nu_1 - \kappa_0\nu_0\rangle = (\kappa_1 - \kappa_0)\,|w|.$$

Since (x_t, y_t) is a minimum of Φ, the left-hand side is nonnegative, giving $\kappa_1 \geq \kappa_0$. □

Lemma 4.3 (Time derivative of the squared distance)**.** *At a minimising pair (x_t, y_t) for $\Phi(\cdot,\cdot,t)$,*

$$\partial_t\Phi(x_t, y_t, t) = \langle w,\, \kappa_1(y_t,t)\nu_1(y_t,t) - \kappa_0(x_t,t)\nu_0(x_t,t)\rangle = (\kappa_1(y_t,t) - \kappa_0(x_t,t))\,|w|.$$

In particular, by Lemma 4.2,

$$\partial_t\Phi(x_t, y_t, t) \;\geq\; 0.$$

Proof. Differentiate Φ in time using $\partial_t\gamma_i = \kappa_i\nu_i$:

$$\partial_t\Phi = \langle \gamma_1 - \gamma_0,\, \partial_t\gamma_1 - \partial_t\gamma_0\rangle = \langle w,\, \kappa_1\nu_1 - \kappa_0\nu_0\rangle.$$

At the minimising pair, $\nu_0 = \nu_1 = w/|w|$ by Lemma 4.1, yielding the formula and the inequality. □

Theorem 4.4 (Avoidance Principle)**.** *Let $\gamma_1, \gamma_2 : S^1 \times [0,T) \to \mathbb{R}^2$ be two smooth embedded curves evolving by curve shortening flow,*

$$\partial_t\gamma_i = \kappa_i\nu_i, \qquad i = 1, 2.$$

If $\gamma_1(\cdot,0)$ and $\gamma_2(\cdot,0)$ are disjoint, then the two curves remain disjoint for all $t > 0$ for as long as both flows exist.

Proof. Set

$$\Phi(x, y, t) := \tfrac{1}{2}\big|\gamma^{(1)}(y,t) - \gamma^{(0)}(x,t)\big|^2 \qquad (x, y \in S^1,\ t \in [0,T)).$$

From Lemma 4.1 there exist (x_t, y_t) attaining the minimum of $\Phi(\cdot,\cdot,t)$, and $\frac{1}{2}d(t)^2 = \Phi(x_t, y_t, t)$.

First-variation at a minimising pair. Let $w := \gamma^{(1)}(y_t,t) - \gamma^{(0)}(x_t,t)$. Stationarity in x and y gives $\langle w, \partial_x\gamma^{(0)}(x_t,t)\rangle = \langle w, \partial_y\gamma^{(1)}(y_t,t)\rangle = 0$, so w is orthogonal to both tangents. Hence the unit tangents are parallel, and we may choose arc-length parameters s, σ near x_t, y_t with unit tangent T_i and unit normal ν_i so that

$$\nu_0(x_t,t) = \nu_1(y_t,t) = \frac{w}{|w|}.$$

Second-variation in space. Using $\partial_s T_i = \kappa_i\nu_i$,

$$0 \leq \partial_{ss}\Phi + \partial_{\sigma\sigma}\Phi = \langle w, \kappa_1\nu_1 - \kappa_0\nu_0\rangle = (\kappa_1 - \kappa_0)\,|w| \quad \text{at } (x_t, y_t, t).$$

Thus

$$\kappa_1(y_t,t) \geq \kappa_0(x_t,t).$$

Time derivative at a minimising pair. By the flow equation $\partial_t\gamma^{(i)} = \kappa_i\nu_i$,

$$\partial_t\Phi(x_t, y_t, t) = \langle w, \partial_t\gamma^{(1)} - \partial_t\gamma^{(0)}\rangle = \langle w, \kappa_1\nu_1 - \kappa_0\nu_0\rangle = (\kappa_1 - \kappa_0)\,|w| \geq 0.$$

Since $\Phi(x_t, y_t, t) = \frac{1}{2}d(t)^2$, we conclude $d(t)$ is nondecreasing.

Avoidance. If $d(0) > 0$, then $d(t) \geq d(0) > 0$ for all $t < T$, so the curves remain disjoint. If at a first time t_* one had $d(t_*) = 0$, the above shows $\partial_t \Phi \geq 0$ and the strong maximum principle implies local coincidence of the flows; by uniqueness for CSF they agree globally, which contradicts disjointness at $t = 0$. Hence avoidance holds. □

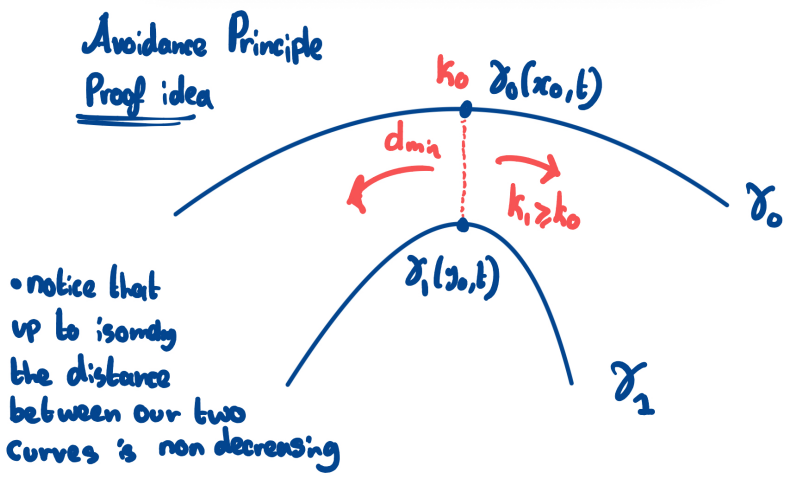

FIGURE 3. Illustration of the avoidance principle. Two initially disjoint curves γ_0 and γ_1 evolve under the flow. At the closest points $\gamma_0(s_a, t)$ and $\gamma_1(s_b, t)$, the distance $d_{\min}$ is non-decreasing in time, ensuring that the curves cannot intersect.

Remark 4.5. This result is the geometric analogue of the parabolic comparison principle: just as sub- and supersolutions of a parabolic PDE cannot cross, two initially disjoint evolving curves cannot newly intersect under curve shortening flow. In particular, embeddedness is preserved for all positive times.

Example 4.6 (Two circles)**.** Let γ_i be circles of radii $r_i(t)$ centered at distinct points. Under curve shortening flow each evolves by $r_i'(t) = -1/r_i(t)$, so their radii decrease while the distance between the centers remains fixed. Hence $d(t) = (\text{center distance}) - (r_0(t) + r_1(t))$ is nondecreasing, illustrating the avoidance principle in a simple symmetric case.

Example 4.7 (Self-avoidance)**.** If one applies the avoidance principle to a curve and a time-shifted copy of itself, one obtains preservation of embeddedness: a simple closed curve under CSF cannot develop self-intersections.

4.2. **Preservation of Convexity.** The avoidance principle ensures that two initially disjoint curves evolving by curve shortening flow remain disjoint for all later times. In particular, applying the principle to a curve and a slightly offset copy of itself shows that the flow preserves *embeddedness*. We now turn to a stronger geometric property that is also preserved: *convexity*.

Intuitively, under the motion $\partial_t \gamma = \kappa \nu$, regions of higher curvature contract more rapidly than flatter parts of the curve, so a nonconvex indentation tends to straighten rather than deepen. One therefore expects that if a curve is convex at the initial time, it remains convex for as long as the flow exists.

Theorem 4.8 (Preservation of convexity)**.** *Let $\gamma(\cdot,t): S^1 \to \mathbb{R}^2$ be a smooth solution to curve shortening flow*

$$\partial_t \gamma = \kappa\, \nu \qquad (t \in [0,T)),$$

with unit tangent $T = \partial_s \gamma$, unit normal ν, and signed curvature $\kappa = \langle \partial_s T, \nu \rangle$. If $\kappa(\cdot,0) > 0$ (i.e. $\gamma(\cdot,0)$ is strictly convex), then

$$\kappa(\cdot,t) > 0 \quad \textit{for all } t \in [0,T),$$

so the evolving curves remain strictly convex. More generally, if $\kappa(\cdot,0) \geq 0$ and $\kappa(\cdot,0) \not\equiv 0$, then $\kappa(\cdot,t) > 0$ for every $t > 0$.

Proof. We use the curvature evolution equation under CSF (with respect to arc-length s):

$$\partial_t \kappa \;=\; \partial_{ss}\kappa \;+\; \kappa^3.$$

Let $\kappa_{\min}(t) := \min_{s \in S^1} \kappa(s,t)$. Since S^1 is compact, $\kappa_{\min}(t)$ is attained. At a spatial minimum point s_t we have $\partial_s \kappa(s_t,t) = 0$ and $\partial_{ss}\kappa(s_t,t) \geq 0$. Evaluating at (s_t,t) gives

$$\partial_t \kappa(s_t,t) \;\geq\; \kappa(s_t,t)^3.$$

Hence the function $m(t) := \kappa_{\min}(t)$ satisfies the differential inequality $m'(t) \geq m(t)^3$ in the viscosity/maximum-principle sense, so $t \mapsto m(t)$ is nondecreasing. If $m(0) > 0$, then $m(t) \geq m(0) > 0$ for all t, proving preservation of strict convexity.

If $\kappa(\cdot,0) \geq 0$ and not identically zero, then either $m(0) > 0$ and we are done, or $m(0) = 0$. In the latter case, the strong maximum principle applied to our curvature evolution equation (a uniformly parabolic scalar equation on the closed manifold S^1) implies that for every $t > 0$ we have $\kappa(\cdot,t) > 0$; otherwise $\kappa(\cdot,t) \equiv 0$ for all t in some interval, which cannot occur for a nontrivial closed curve evolving by CSF. □

Remark 4.9 (Evolution identities used). With $T = \partial_s \gamma$ and ν the unit normal, the standard CSF identities are

$$[\partial_t, \partial_s] = \kappa^2 \partial_s, \qquad \partial_t T = \partial_s(\kappa \nu) = \kappa_s \nu - \kappa^2 T, \qquad \partial_t \nu = -\kappa_s T,$$

and

$$\kappa = \langle \partial_s T, \nu \rangle \;\Rightarrow\; \partial_t \kappa = \partial_{ss}\kappa + \kappa^3.$$

These should be familiar from the proof of the avoidance principle. In fact this is just another way to derive the curvature evolution equation.

Remark 4.10 (Geometric consequences). The avoidance and convexity results together provide a complete qualitative picture of the planar curve shortening flow. The avoidance principle ensures that embedded curves cannot newly intersect, so the topology of each component of the flow is preserved. Meanwhile, the preservation of convexity guarantees that the geometric shape of a convex curve improves monotonically, becoming more circular as time progresses. In combination, these two principles imply that every embedded curve evolves smoothly without developing singularities of intersection or loss of convexity before extinction.

4.3. **Discussion and Further Consequences.** The results of this section illustrate the power of the parabolic maximum principle when translated into a geometric setting. Analytic properties of the curvature equation,

$$\partial_t \kappa = \kappa_{ss} + \kappa^3,$$

manifest directly as geometric invariants of the evolving curve.

(1) Topological preservation. The avoidance principle is the geometric analogue of the parabolic comparison principle: two distinct "solutions" (curves) cannot cross. Consequently, the topology of the flow is fixed from the initial configuration—embedded curves remain embedded, and disjoint families of curves stay disjoint for all positive times.

(2) Monotone improvement of shape. The preservation of convexity follows from the strong maximum principle applied to the curvature equation. It ensures that curvature remains positive, so convexity is retained and, in fact, enhanced under the flow. Regions of higher curvature contract more rapidly, causing the curve to become rounder over time.

(3) Approach to circularity. These principles together imply that a convex embedded curve evolves smoothly toward a round point. Quantitatively, this behaviour is captured in the classical results of Gage and Hamilton Gage and Hamilton [3] and Grayson Grayson [4], which show that the normalised curve converges exponentially to a circle before extinction.

In summary, the analytic tools developed in Section 2—comparison and maximum principles—translate under curve shortening flow into geometric statements of disjointness, convexity, and monotonic smoothing. They form the core analytical foundation for understanding the long-time and asymptotic behaviour of CSF. In the next section, we explore another fundamental parabolic phenomenon, the *infinite propagation speed*, and interpret its geometric meaning in the context of curve evolution.

5. Infinite Propagation Speed and Smoothing

The parabolic nature of the curve shortening flow ensures not only geometric monotonicity but also instantaneous regularization of the evolving curve. We now examine the phenomenon of *infinite propagation speed* and the associated smoothing effects, before describing the finite-time extinction and asymptotic self-similarity of the flow.

5.1. **Infinite propagation speed.** For the one-dimensional heat equation

$$u_t = u_{xx},$$

a local disturbance in $u(x, 0)$ affects $u(x, t)$ at every spatial point for all $t > 0$. The curvature evolution equation

$$\kappa_t = \kappa_{ss} + \kappa^3$$

is quasilinear but uniformly parabolic wherever κ is bounded, since the principal term κ_{ss} dominates for small times. Consequently, the equation exhibits the qualitative feature of *infinite propagation speed*: local variations in curvature are instantaneously felt along the entire curve.

If $\kappa(\cdot,0)$ is merely continuous, the parabolic maximum principle implies

$$\inf_{S^1}\kappa(\cdot,0)\leq\kappa(s,t)\leq\sup_{S^1}\kappa(\cdot,0),\qquad\forall t>0,$$

while higher-order regularity follows from standard parabolic bootstrapping (see Evans Evans [2], §11.1, or Lieberman Lieberman [5]). Hence any weakly regular or nonsmooth initial curvature becomes instantly C^∞ for $t>0$. Geometrically, corners, kinks, and oscillations of the initial curve γ_0 are immediately smoothed—the curve becomes analytic for all positive times.

Remark 5.1. The term *infinite propagation speed* refers to the fact that, for uniformly parabolic equations, perturbations in the initial data are felt immediately throughout the domain, in contrast to hyperbolic equations, which exhibit finite propagation speed.

5.2. **Broader significance.** The qualitative behaviour of CSF—avoidance, convexity preservation, instantaneous smoothing, and circular collapse—arises solely from parabolic analytic principles. The maximum and comparison principles translate into geometric disjointness and convexity, while diffusion and infinite propagation yield global regularization. These mechanisms reappear in higher-dimensional flows: the mean curvature flow of hypersurfaces and Hamilton's Ricci flow on manifolds share the same parabolic structure and exhibit analogous smoothing and monotonicity phenomena. Thus, CSF provides a minimal yet complete model for understanding how analytic features of parabolic PDEs govern geometric evolution.

5.3. **Conclusion.** The curvature equation

$$\kappa_t=\kappa_{ss}+\kappa^3$$

encodes the essential bridge between analysis and geometry.

$$\begin{aligned}\text{Comparison principle}&\implies\text{Avoidance of intersections},\\ \text{Strong maximum principle}&\implies\text{Preservation of convexity},\\ \text{Infinite propagation speed}&\implies\text{Instantaneous smoothing},\\ \text{Scaling invariance}&\implies\text{Self-similar circular collapse}.\end{aligned}$$

Hence every smooth embedded planar curve under curve shortening flow remains embedded, becomes convex, and shrinks in finite time to a round point. The CSF therefore stands as the prototypical example of how parabolic partial differential equations dictate geometric evolution.

6. Further Directions – A Note on Grayson's Theorem

The results obtained so far describe the local and qualitative behaviour of the curve shortening flow: embedded curves remain embedded, convexity is preserved, and convex curves shrink smoothly to round points. A natural question remains: does this picture hold for *all* embedded curves, not only those that are initially convex? This question marks the transition from local analysis to a global geometric classification, and its resolution represents the culmination of the entire theory of planar curve shortening flow.

The answer, due to Matthew A. Grayson in a landmark 1987 paper, is strikingly clear. *Every smooth embedded curve in the plane becomes convex in finite time and then contracts to a round*

point under the flow. Grayson's theorem unifies all the analytical principles developed so far—comparison, maximum, and smoothing—into a single global statement. It shows that the curve shortening flow acts as a perfect geometric regulariser: any embedded curve, no matter how intricate, evolves through progressively smoother and simpler shapes until it becomes circular and vanishes. In this sense, Grayson's result stands as the definitive conclusion of the study of CSF, transforming local differential principles into a complete global description of geometric evolution.

6.1. **Grayson's theorem.**

Theorem 6.1 (Grayson, 1987 Grayson [4])**.** *Every smooth embedded closed curve in the plane evolving by curve shortening flow becomes convex in finite time and, once convex, remains convex until it shrinks to a round point.*

Grayson's theorem provides a definitive classification of the long-time behaviour of planar CSF. It establishes that convexity is not merely preserved but is, in fact, an *attractor property* of the flow: for any embedded initial curve, the evolving family γ_t becomes convex before extinction. Combining this with the result of Gage and Hamilton Gage and Hamilton [3], who proved the convex case, yields a complete description of the planar flow:

$$\text{any embedded curve} \quad \Longrightarrow \quad \text{convex curve} \quad \Longrightarrow \quad \text{round point.}$$

Hence, the curve shortening flow serves as a geometric regularisation mechanism that transforms arbitrary embedded shapes into perfectly circular singularities. From the analytic viewpoint, Grayson's theorem can be interpreted as a global convergence result for the nonlinear parabolic PDE

$$\kappa_t = \kappa_{ss} + \kappa^3,$$

demonstrating that the only asymptotically stable stationary solution (up to scaling) is $\kappa \equiv 1$. This result elegantly completes the analytic and geometric understanding of CSF, showing how local parabolic behaviour culminates in global regularity and classification.

6.2. **Historical note and outlook.** The progression from the convex case studied by Gage and Hamilton Gage and Hamilton [3] to Grayson's general theorem Grayson [4] represents one of the most elegant developments in geometric analysis. Gage and Hamilton first proved that convex curves remain convex and shrink smoothly to round points, establishing the analytic foundations for curvature evolution and the use of maximum principles. Building on this framework, Grayson removed the convexity assumption entirely, showing that every embedded curve eventually becomes convex before collapsing to a round point. Together, these two results complete the classification of planar curve shortening flow, marking a rare instance in geometric PDE theory where a nonlinear evolution is completely understood from initial data to singularity.

Beyond the plane, similar principles guide the mean curvature flow of hypersurfaces and the Ricci flow on manifolds, where convexity and monotonicity remain central but singularities become far more complex. The curve shortening flow thus serves as a foundational model for geometric evolution equations, illustrating how analytic tools—comparison principles, parabolic regularity, and self-similar rescaling—combine to reveal deep structure in the geometry of evolving shapes.

Acknowledgements

I thank Professor Raphael Zentner for his supervision, guidance, and incredible generosity on this project. I would also likely to dedicate this to Neil Hankinson. May he rest in peace.

References

[1] Bennett Chow and Dan Knopf. *Extrinsic Geometric Flows*, volume 135 of *Mathematical Surveys and Monographs*. American Mathematical Society, Providence, RI, 2004.

[2] Lawrence C. Evans. *Partial Differential Equations*. American Mathematical Society, 2nd edition, 2010.

[3] Michael E. Gage and Richard S. Hamilton. The heat equation shrinking convex plane curves. *Journal of Differential Geometry*, 23(1):69–96, 1986.

[4] Matthew A. Grayson. The heat equation shrinks embedded plane curves to round points. *Journal of Differential Geometry*, 26(2):285–314, 1987.

[5] Gary M. Lieberman. *Second Order Parabolic Differential Equations*. World Scientific, 1996.